Prototype Optical Modelling Procedure and Outdoor Characterization of an Embedded Polyolefin Crossed Compound Parabolic Concentrator for Integrated Photovoltaic Windows

Katie Shanks[1, a)] Ashley Knowles[2], Adam Brierly[3], Hasan Baig[1, b)], Yanyi Sun[4], Yupeng Wu[4], and Tapas Mallick[1, c)]

[1]*Environment and Sustainability Institute, University of Exeter Penryn Campus, TR10 9FE, Cornwall, UK.* [2]*Yorkshire Photonics, Halifax, HX3 6SN, UK.* [3]*Brinell Vision, Dundee, DD1 5JJ, UK.* [4]*Architecture and Built Environment, Faculty of Engineering, University of Nottingham, Nottingham, NG7 2RD, UK.*

[a)]Corresponding author: K.Shanks2@exeter.ac.uk

Abstract. We present a method to optically model prototypes pre- and post-manufacturing to incorporate material flaws and understand clearly the potential of designs at the prototyping stage of window integrated PV systems. A prototype Window Embedded Crossed Compound Parabolic Concentrator (WE-CCPC) made of plastic Topaz optics, arrayed within double glazed windows as a means to provide both electricity and natural sunlight to a building is presented. The outdoor performance of the prototype is characterized, and the theoretical and experimental results compared. The manufactured module was found to have an optical efficiency of 77% at normal incidence and an acceptance angle of 20° once realistic material and manufacturing considerations were incorporated. Optical losses such as the absorption, cell reflectance, slope errors and irradiance nonuniformity were found to decrease the acceptance angle significantly as all increase with increased incidence angle, accumulating to the ~15° of acceptance angle loss from the original modelling.

INTRODUCTION

Concentrator photovoltaic (CPV) systems reduce the requirement of photovoltaic materials needed in a system installation [1]. This in turn reduces the carbon footprint of making this type of solar energy technology and can also reduce the cost of the system whilst maintaining or even increasing the power output. Despite these advantages, CPV costs limit the technologies competitiveness with flat plate silicon panels. Applications where space is limited and energy demand is high, such as for domestic use, are where CPV technology may contend, especially if more interesting, aesthetically pleasing designs are desired. CPV technology also has the advantage of being flexible in its size, shape and transparency. Recent market research suggests that for CPV to succeed alongside standard flat plate PV, niche applications such as building integration, using embedded systems, need to be developed [2]. There is much potential for smart integrated solar windows [3] with many designs, materials and manufacturing processes in need of investigation. Thus, we present a method to optically model prototypes pre- and post-manufacturing in order to incorporate manufacturing flaws and understand clearly the potential of designs at the prototyping stage. The optical modelling completed was that of Monte-Carlo Ray Tracing but even within this method, and specifically for individual software (e.g. Optisworks, TracePro, Zemax, Breaults ASAP and APEX etc...), the methods to accurately model the materials, geometry and light properties can vary substantially. Here we outline the steps and the software's functions of the optical modelling with which initial variables are required and should be altered after measurements of the manufactured components can be made.

The prototype used is a window embedded crossed compound parabolic concentrator (WE-CCPC) prototype made of plastic 'Topas' (Polyolefin/Zeonex: COC Polymer), arrayed within double glazed windows as a means to

provide both electricity and natural sunlight to a building. The Polyolefin optics were found to double the power to weight ratio of a standard silicon solar cell and were half the weight of the glass optic counterpart device measured. The outdoor performance of the prototype is characterised and presented here, discussing the performance due to sun angle for a south facing vertical WE-CCPC prototype.

Design of Window Embedded Crossed Compound Parabolic Concentrator (WE-CCPC)

The low concentration optic chosen for this window embedded system was the crossed compound parabolic concentrator (CCPC) which has been previously optimized by Hasan et.al.[4] for a wide acceptance angle of ~35°.

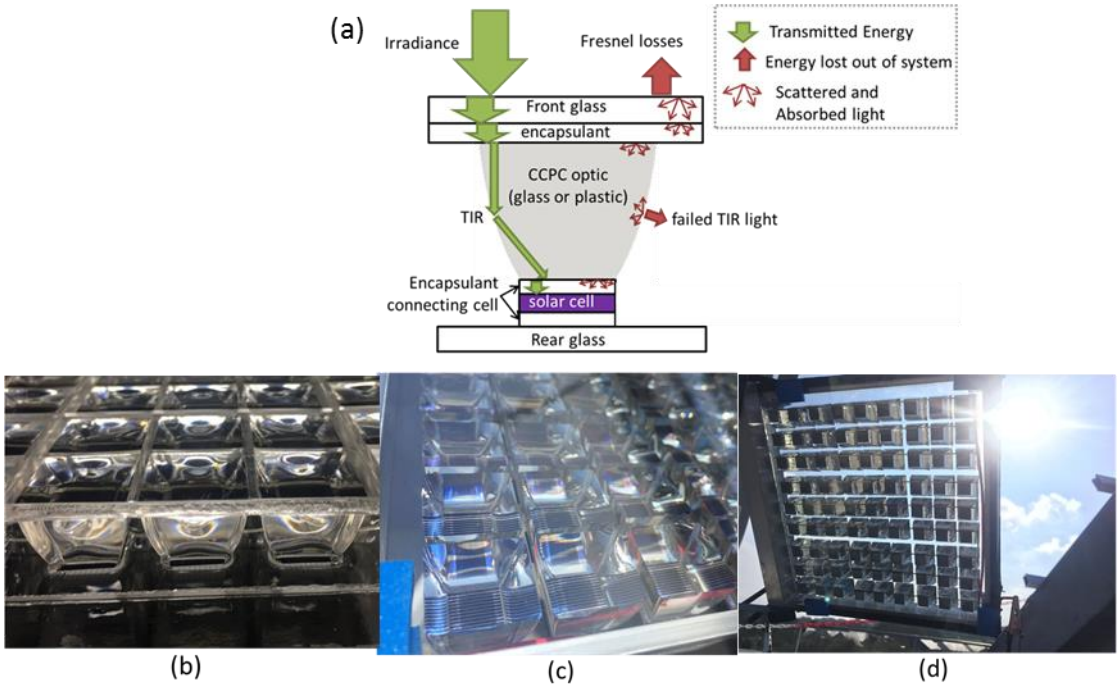

FIGURE 1. (a) Diagram of Crossed Compound Parabolic Concentrator (CCPC) embedded within double glazing. Energy progression and loss in the system shown. (b) Plastic 'Topas' optics manufactured from injection mold array. (c) Window Embedded CCPC top view and (d) Back view of Window Embedded CCPC prototype outdoors.

As can be seen from Figures 1(a)-(d) some of the light will concentrate towards the cell and some will pass through the window system. Thus, the 'lost' light (Figure 1(a)) will be useful by contributing to the lighting of a room. The prototypes developed in this study (Figures 1 b-d) obtain maximum compactness and electricity production. The main applications in mind being: sky lighting in roofs; office skyscrapers made of large area double glazed walls (opportunities to reduce glare and AC) and rain shelters. Further analysis of this system concept, design and analysis is reported elsewhere [5] with further investigations to follow.

OPTICAL MODELLING METHOD

Accurately modelling optical systems for concentrator photovoltaic (CPV) designs is an important step in prototyping and developing CPV technology. The materials chosen at the prototyping stage may differ or not be known at the initial optical design stage and hence optical modelling should be adjusted to allow accurate analysis of the losses within the built system. Such losses to be considered which vary with specific material and manufacturing choice are absorption, surface scattering and slope errors. Surface scattering and specific slope errors can increase unwanted Fresnel reflections and decrease desired reflective/refractive performance. Manufacturing methods each

come with their own surface quality. Re-modelling these flaws into the optical model allows clear understanding of the realistic performance of the CPV design and how much further the built system can be improved under scaled commercial manufacturing. The optical modelling presented here uses Monte-Carlo Ray tracing carried out within the Breault ASAP software and incorporates the material absorption for 'Topas' (Polyolefin/Zeonex) as well as the surface quality resultant from injection molded optical arrays with slight slope defects due to material shrinkage.

The components, input parameters and output parameters of a CPV optical model are shown in Figure 2. These are ordered by the optical losses introduced to the system - in complexity and accuracy of the optical losses included. Due to the complexity and variability of CPV designs, methods are presented as general variables. There is a need for further standardization in CPV theory, here, 'geometrical losses' will refer to optical losses occurring only due to the shape and simplified refractive index of the optics. No absorption, Fresnel reflection or scattering will be accounted for, and the optical shapes can be assumed perfect for this design stage 1. This stage allows for initial limits and known parameters to be implemented, taking n=1.5 for refractive optical components and ensuring the incident light has a divergence angle of ±0.27degrees [1]. The solar divergence angle is important to include at the geometrical design stage 1 as it dictates the maximum concentration limits for CPV systems [1]. Typical known parameters are be the PV cell response range, the geometric concentration ratio desired (this may be increased to allow for losses) and the maximum input aperture size allowed for a specific application. Knowing the working wavelength range of the cell (e.g. 350-1100 for Silicon) allows selection of the light source wavelength range to be simulated. For thermal modelling of the PV cell, other wavelengths should be used and the optical output can be used as the input to a thermal model. Stage 1 optical modelling also allows checking the software and method being used for errors, this stage should allow 100% efficiency as long as the design geometry allows it in theory. This may be important for finding the most suitable concentration ratio and CPV system type (e.g. Fresnel lens, Cassegrain).

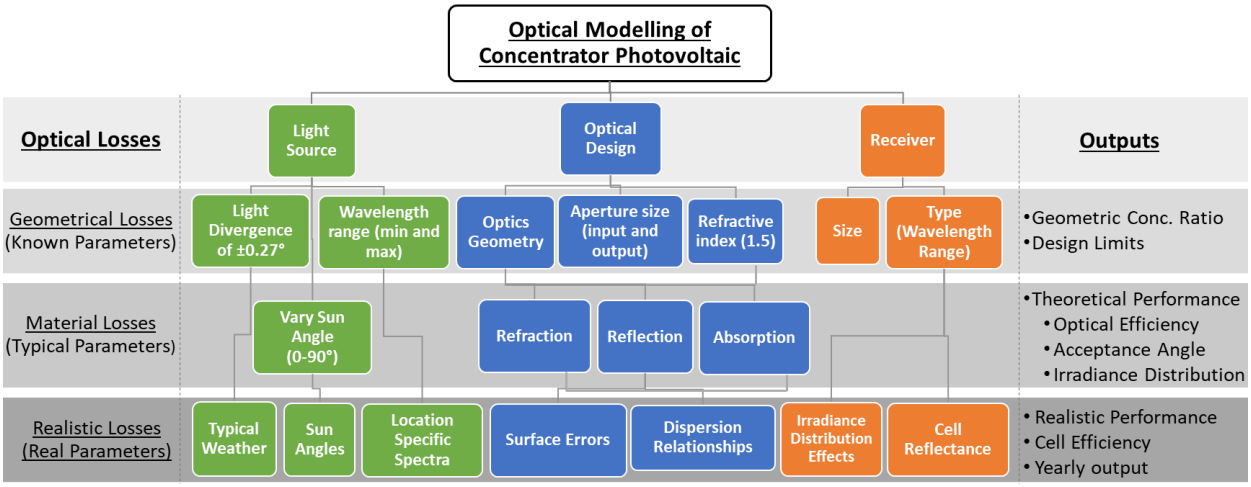

FIGURE 2. Flow chart of optical losses, modelling input considerations and types of outputs at each stage of optical modelling to achieve accurate analytical results. Input parameters classified within subsystems of light source, optical design and receiver.

The next design stage should include assumed material optical efficiencies provided by the literature. This may include 90-95% reflective mirrors and ~5% Fresnel reflection loss at glass/air interfaces. The refractive index of the lens components is still assumed n=1.5 from stage 1. These typical material properties can be included and modelled by various methods [6]–[10]. The simplest is to include the optical loss (absorption, Fresnel reflection etc.) as single value losses applied in the same magnitude to every ray. This would have the same effect as simply multiplying stage 1's geometric optical efficiency by the transmittance and reflectance of the components within the design and can be done within the software by attributing these efficiencies to a component or interface. This however is not the case as some rays will experience varying degrees of these optical losses depending on their wavelength, incidence angle and path length (absorbing medium). Ray trace software can easily incorporate more accurate weighting, typically by assigning material properties to components and interfaces which will follow fundamental relationships

between incidence angle, refractive index and wavelength [7], [10]. For example, for Fresnel reflections, the proportion of an incident light ray refracting and reflecting can be calculated through Fresnel equations within the software. Again, within the software it can usually be decided if this be done for a specified 'average' wavelength or calculated for each individual light rays wavelength and incidence angle within the given environment (simulation set up parameters). This of course increases simulation processing time which can be very long for very large complex systems (e.g. including a Fresnel lens with many discrete facets). The next additional complexity is the surface roughness of the material. This in particular can be simulated in even more ways and adds further processing time [6], [7], [9], but perhaps these levels of accuracy are not required at this stage of the optical modelling as they will be inaccurate regardless without the exact material and manufacturing properties known. Typically these attributes, with resultant surface quality and hence optical efficiency, of each component is not known at this stage but an optimized design is required to discuss with manufacturers for price. Hence, it is common at stage 2 for the simpler, less accurate ray tracing parameters to be used. For this case, the wavelength and angle dependent Fresnel calculations with the wavelength dependent PMMA transmittance (figure 3a) multiplication for the CCPC lens were incorporated. These combined with varying the effective solar angle between 0-90 degrees gives the stage 2 results in figure 3. Depending on the application, the design may be optimized for acceptance angle, optical efficiency, irradiance distribution, minimum weight, compactness or simplicity and this stage can decide CPV type (e.g. lens).

Following the first and second optical modelling stages obtains the optimized CCPC of ~16mm height, 3.6 suns geometric concentration ratio and acceptance angle ~35° [4], its performance shown in Figure 3. The absorption of PMMA was included in the second stage of modelling to gain an idea of the main loss of such a bulk refractive optic. PMMA and PC are the most commonly used CPV materials and there transmittance reported repeatedly in the literature and hence is usually available in ray tracing software. However, the high transmittance range of both PMMA and PC only begins at ~360nm which for the Silicon solar cell can bring the average transmittance down substantially (~9% loss). The injection moldable material 'Topas' (Polyolefin/Zeonex: COC Polymer) was found to have the highest transmittance over the full silicon cell wavelength range (300-1100nm) out of the materials tried, molded and tested within this study. As can be seen from figure 3a, PMMA is likely more suitable for CPV systems incorporating multijunction solar cells but for single junction silicon, the lower long wavelength transmittance could be beneficial for the cells efficiency. Overall, investigating this COC Polymer was more advantageous for higher performance and expanding material understanding for low concentration CPV's.

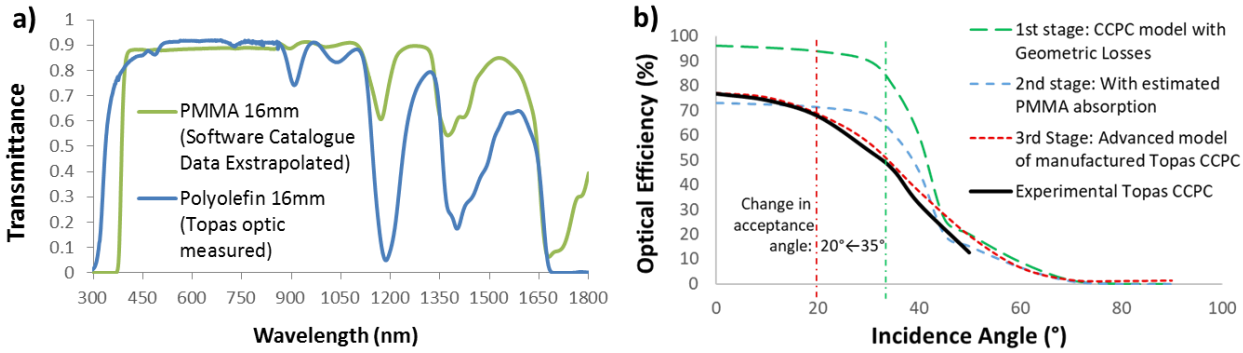

FIGURE 3. a) Transmittance of 16mm thick PMMA and Polyolefin 'Topas'. b) Theoretical and experimental performance of CCPC for increased angles of incident light detailing 3 stages of optical modelling proposed.

Due to the bulk volume of the CCPC optic (regardless of material chosen), natural cooling of the optics after injection molding caused an inwards shrinkage as the inner material cooled much slower than the outer surface material. This caused slope errors as can be seen in Figure 1b. The surface smoothness however from these injection molded optics was very good such that surface scattering due to surface roughness would be minimal. A Lehr (moving belt) set up taking the fresh injection molded optics gradually through lower temperature oven zones would eliminate this error in scaled manufacturing but for these prototyping investigations this was not possible.

Experimental surface tests using monochromatic light comparing the reflection efficiency of a correctly curved surface and deformed curved surface suggested a ~2% energy loss per incident light ray. This was confirmed in the ray trace simulation by incorporating not only scattering losses over all the surfaces of the CCPC geometry but also altering the geometry to include a central inward shallow cone at the center of each CCPC side wall which ranged in depth such that 1-10% additional losses were seen per side wall shrinkage. The appropriate shrinkage depth was

chosen by analyzing light loss for a small cluster of incident rays upon the side wall area and comparing with measured results. The advanced optical modelling stage incorporated 5 additional losses: 1. The absorption of Polyolefin, which also increases with incidence angle due to increased light ray path lengths within the material. 2. The slope error losses which have more impact with increased incidence angle as more light rays hit the deformed side walls of the CCPC. 3. Light lost at the edges of the optics base where encapsulant slightly overlaps the optic to join the cell [4]. 4. Cell reflection losses which also increase with increased incidence angle. 5. Estimated irradiance distribution losses which again are most influential at increased incidence angles [11]. This 3rd stage optical modelling gave the most accurate CCPC optical efficiency prediction as a function of incidence angle as shown in figure 3. There is still a very slight overestimation which can be attributed to current mismatch between optics as the tested system was of 9 units connected in series. The absorption was modelled using 3D volumetric absorption functions. This essentially calculated the path length of each ray, including scattered split off rays, within the CCPC volume limits and assigned a final magnitude (following the beer-lambert relationship) to rays escaping the CCPC bounds. The simulation time of this type of calculation can be helped by giving a cut off to rays that undergo too many reflections/interface interactions or discontinuing their 'tracking' once their magnitude falls below a certain negligible value which may have contributed to the overestimation in figure 3b. The scattering and slope errors were simulated by assigning Bi-directional Scatter Distribution Functions (BSDF) to each surface of the CCPC geometry [7]. As stated previously this varies itself, between isotropic (uniform roughness/scattering across surface) and anisotropic (non-uniform but ordered errors such as parallel brush marks and CNC grooves[7]) scatter models which can then be subcategorized further into Lambertian, Harvey, RMS, Nonlinear, Viened, Volume, Cavity, Bionomial etc. [7]. The modified Harvey isotropic scattering model was utilized here with values available within the software for polished molded acrylic type optics. The encapsulant overlap was simulated by including overlapping interfaces with refractive index 1.42 (Sylgard 184) and the cell reflectance values added manually (User defined data file) using measured data that gives the reflectance dependent on wavelength and angle of incidence. The irradiance distribution losses were only estimated as a single value loss independent of wavelength but which increased with incidence angle following previous studies [11].

OUTDOOR CHARACTERIZATION

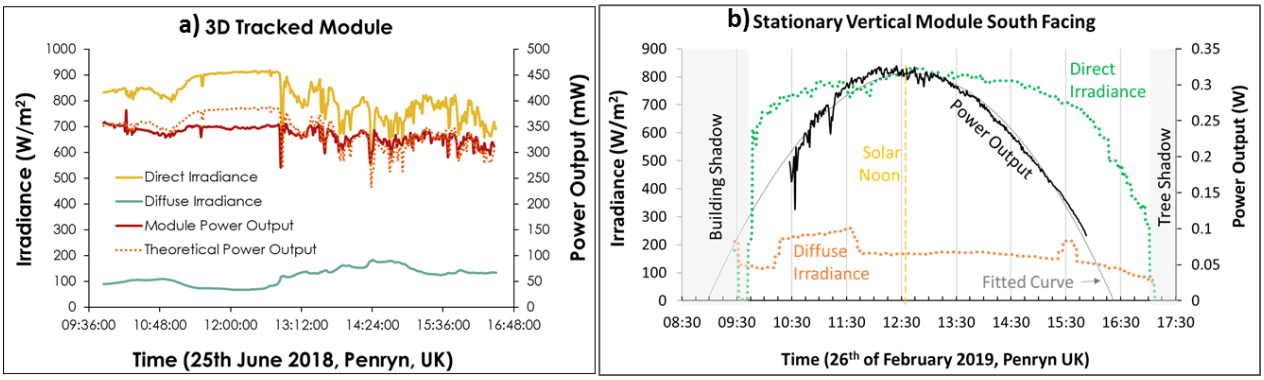

FIGURE 4. a) Dual-Axis tracked outdoor measurements on the 25th of June 2018 in Penryn, UK, showing the direct irradiance, diffuse irradiance and power output from the WE-CCPC prototype. b) Stationary WE-CCPC prototype positioned vertical and south facing. Outdoor measurements recorded on the 26th of February 2019 in Penryn, UK

Prototypes of the CCPC's embedded within a double-glazed window were manufactured (Figure 1) and tested outdoors (Figures 4 and 5). For proof of performance and to obtain maximum power capabilities, Figure 4 shows the dual-axis tracked performance of the module. Figure 5 shows the realistic performance of a module installed vertically, such as the case for a window, facing south to easier investigate sun angle effects on the module performance. The output power can be seen to follow the direct irradiance and the theoretical prediction with a strong dependence as expected but with a significant loss over the longest uninterrupted peak irradiance over solar noon. This is expected to be due to the cell temperature increasing significantly and reducing the cell efficiency which was not incorporated in the theoretical calculations, but which is widely studied elsewhere [12].

In a real installation scenario however, the solar cells would not be subject to such a prolonged peak irradiance due to their fixed position but would be dependent on the suns position in relation to the modules orientation. For a vertical WE-CCPC module facing south (figure4b), the peak performance would be at Solar Noon with a symmetrical profile on either side following the suns motion across the sky as it passes across the optics acceptance angle as in figure 5b.

CONCLUSION

A window embedded compound parabolic concentrator module is presented, the optical losses modelled accurately using measured component performance feedback into the simulation, and the outdoor performance given for a tracked and stationary device. Thorough considerations of the realistic errors, including slope deformation due to bulk material shrinkage, allows an accurate understanding of the CCPC performance and its reduced acceptance angle from the designed optimum. The manufactured 'Topas' (Polyolefin/Zeonex: COC Polymer) CCPC has an acceptance angle of 20° instead of the designed 35° due to optical losses of absorption, cell reflection, slope error and irradiance non-uniformity which all increase with increased incidence angle, reducing the realistic acceptance angle. The outdoor characterisation confirmed the advanced post manufacturing modelling procedure to be accurate, only missing the cell temperature considerations and small mismatch losses in a series connection of unit devices. The WE-CCPC performance during a day will depend on the building orientation in relation to the sun but the window opening mechanism could be chosen to improve this.

ACKNOWLEDGMENTS

This work is funded by Innovate UK through the E-IPB project. Authors acknowledge all funding agencies for the support. In support of open access research all underlying article materials (such as data, samples or models) can be accessed upon request via email to the corresponding author.

REFERENCES

1. P. Perez-Higueras and E. F. Fernandez, *High Concentrator Photovoltaics: Fundamentals, Engineering and Power Plants*, 1st ed. Jaen: Springer International Publishing, 2015.
2. J. P. Morgan, "Why Hasn't CPV Taken Off Yet and Will the Future Look Different," in *AIP-13th International Conference on Conentrator Photovoltaic Systems (CPV-13)*, 2017.
3. Y. Wu, K. Connelly, Y. Liu, X. Gu, Y. Gao, and G. Z. Chen, "Smart solar concentrators for building integrated photovoltaic façades," *Sol. Energy*, vol. 133, pp. 111–118, Aug. 2016.
4. H. Baig, N. Sellami, and T. K. Mallick, "Trapping light escaping from the edges of the optical element in a Concentrating Photovoltaic system," *Energy Convers. Manag.*, vol. 90, pp. 238–246, 2015.
5. N. Kincaid, G. Mungas, N. Kramer, M. Wagner, and G. Zhu, "An optical performance comparison of three concentrating solar power collector designs in linear Fresnel, parabolic trough, and central receiver," *Appl. Energy*, vol. 231, pp. 1109–1121, Dec. 2018.
6. P. Good et. al. "Spectral reflectance, transmittance, and angular scattering of materials for solar concentrators," *Sol. Energy Mater. Sol. Cells*, vol. 144, pp. 509–522, Jan. 2016.
7. Breault Research Organization, "ASAP Technical Guide: Scattering in ASAP," 2012. [Online]. Available: http://www.breault.com/sites/default/files/knowledge_base/brotg0922_scatter_1.pdf. [Accessed: 12-Oct-2015].
8. K. Shanks et. al. "Conjugate refractive–reflective homogeniser in a 500× Cassegrain concentrator: design and limits," *IET Renew. Power Gener.*, vol. 10, no. 4 (PVSAT-11), pp. 440–447, Apr. 2016.
9. S. Schröder, A. Duparré, L. Coriand, A. Tünnermann, D. H. Penalver, and J. E. Harvey, "Modeling of light scattering in different regimes of surface roughness.," *Opt. Express*, vol. 19, no. 10, pp. 9820–9835, 2011.
10. S. A. Miller, J. Pond, L. Solutions, and C. B. Michel, "Raytracing meets Maxwell's Equations integrating micro- and macro-optical design," 2006.
11. H. Baig, N. Sellami, D. Chemisana, J. Rosell, and T. K. Mallick, "Performance analysis of a dielectric based 3D building integrated concentrating photovoltaic system," *Sol. Energy*, vol. 103, pp. 525–540, 2014.
12. I. García, M. Victoria, and I. Antón, "Temperature Effects on CPV Solar Cells, Optics and Modules," in *Handbook of Concentrator Photovoltaic Technology*, Chichester, West Sussex: John Wiley & Sons, Ltd, 2016, pp. 245–292.